



# Surface Integrity and Wear Resistance of Maraging Steel Produced by Additive Manufacturing Direct Metal Laser Sintering

Tolga Berkay Şirin<sup>1</sup> and Yusuf Kaynak<sup>2</sup>

<sup>1</sup>Department of Mechanical Engineering, Institute of Pure and Applied Science, Marmara University, 34722 Istanbul, Turkey

<sup>2</sup>Department of Mechanical Engineering, Technology Faculty, Marmara University, 34722 Istanbul, Turkey

Received: 15.08.2020

Accepted: 27.09.2020

---

## Abstract

This study presents the surface integrity characteristics and wear resistance of maraging steel specimen fabricated by additive manufacturing (AM) direct metal laser sintering (DMLS). After AM process, as-built maraging steels were heat treated by aging 490°C/3h and followed by air cooling. The specimen produced by DMLS were examined considering scanning and building area and compared with the same heat treated wrought specimen in terms of surface integrity aspects and wear resistance. Surface roughness, surface topography, microhardness and XRD analysis tests were performed to evaluate surface integrity properties of these specimens. In addition, the specimens produced by DMLS and the heat treated wrought were compared in terms of wear resistance. Our study illustrates that the wear resistance of the specimen produced by DMLS does not depend on the fabrication directions. Besides, this study revealed that specimens produced by DMLS have much higher wear resistance than wrought ones.

**Keywords:** *Direct Metal Laser Sintering, Maraging Steel, Wear Resistance, Surface Integrity Aspects, Additive Manufacturing.*

---

## 1. Introduction

Maraging steels, which are among the iron-based alloys, combine good material properties such as ultra-high strength, superior toughness characteristics, good weldability and dimensional stability during aging heat treatment [1, 2]. These steels are a special class of low-carbon ultra-high-strength steels [3]. Derive their strength not from carbon, but from hardened by precipitation of intermetallic compounds [4]. In this way, defects such as quench cracking in carbon steel are prevented, while high nickel content and lack of carbide increase the corrosion resistance and gain good machinability by means of low carbon content [5]. Due to such superior properties, they are mainly used in industries such as aircraft and aerospace, machinery and tooling, ordnance components and fasteners, but are also used in the production of industry and engineering parts; rocket engine castings, drill chucks, extrusion, plastics injection molds and metal casting dies [6].

Direct Metal Laser Sintering (DMLS) is one of the most useful laser powder bed fusion methods for metal additive manufacturing [7]. This method is distinguished by the fact that it prevents the formation of residual stresses and internal defects in the produced parts [8]. In addition to the variety of materials to be used in this production method, it is also preferred to offer dense, high strength,

\*Corresponding author: Tolga Berkay Şirin

E-mail: [tolgasirin@marun.edu.tr](mailto:tolgasirin@marun.edu.tr) / ORCID: 0000-0002-5558-1071

functional and corrosive resistance parts which can be treated more by heat, coating and sterilization [9].

Although additive manufacturing processes including laser powder bed fusion provides great benefits comparing with conventional manufacturing process, surface and subsurface characteristics, namely surface integrity of metal components fabricated by additive manufacturing still have some serious problems [10]. Thus post processing operations including heat treatment are commonly used to improve surface quality [11] and wear resistance of specimens fabricated by additive manufacturing process [12]. These studies also confirm that post-processing conditions play a critical role to determine the final surface properties of metal specimens fabricated by additive manufacturing process.

In the literature, there are studies on the additive manufacturing of this particular material, however, no extensive research on surface integrity and wear resistance of the produced by DMLS and compared with wrought and heat treated maraging steel alloy [13, 14]. Thus, this current paper focuses on surface properties of scanning and building area of the maraging steel produced by DMLS and these two were also compared with as received wrought and heat treated wrought specimen in terms of surface, microstructure, and wear resistance.

## 2. Materials And Methods

Specimens are produced with direct metal laser sintering technology by the ProX DMP 200 machine with shape of a rectangular prism with the dimensions of 35x31x31 mm as shown in Figure 1. The detail of AM process parameters were presented in elsewhere [15]. The machine uses a fiber laser with a maximum laser output power of 300W and a wavelength of 1070 nm. The nominal composition of provided maraging steel by 3D Systems is given in Table 1. All specimens produced by DMLS were heat treated. AM specimens were hardened by the subsequent aging method (precipitation hardening at 490°C for 3h, followed by air cooling to room temperature). It should be also noted that wrought specimens have two conditions. One was heat treated following same conditions AM specimens were subjected to. These specimens named wrought & Heat Treated in the rest of the paper. As-received wrought specimen were also analyzed and presented in some part of this study and named as wrought specimen.



**Figure 1.** The image of specimen produced by DMLS method

**Table 1.** Chemical composition of maraging steel produced by DMLS

Alloying Element	Fe	Ni	Co	Mo	Ti	Si	Mn	C
Wt %	rest	17.0-19.0	9.0-11.0	4.0-6.0	0.9-1.0	≤ 1.0	≤ 1.0	≤ 0.003

The specimen was cut using diamond discs to examine the surface characteristics with the Microtest Multicut Sense precision cutting device. Surface roughness values in the scanning and building area were measured on Mitutoyo SJ210 with mean of 10 measurements. Surface topography and microstructure images were visualized by the VHX-6000 Keyence Digital Optic Microscope. The microhardness of the parts was measured using the Future-Tech FM310e. X-ray diffraction (XRD) phase transformations of specimen were analyzed using the Bruker XRD device. Wear tests were performed with reciprocation wear device and friction coefficients were obtained.

### 3. Results and Discussions

#### 3.1 Surface Roughness and Topography

One of the most important problems in the specimens produced by the additive manufacturing is the poor surface quality [16]. The reasons for the poor quality of this specimen are the inability to optimize the production parameters, size of the powder, machine capacity and the operating logic etc.[17, 18]. Figure 2 shows the scanning and building area topography images of the maraging steel produced by DMSL and Figure 3 shows the surface roughness of the specimen in the building and scanning area. Unmelted metal powders in the building area and gaps between the layers have caused higher surface roughness in the building area than scanning area [19]. The surface roughness values (arithmetical mean roughness value, Ra) of the scanning and building area are  $5.1\ \mu\text{m}$  and  $10.5\ \mu\text{m}$ , respectively.

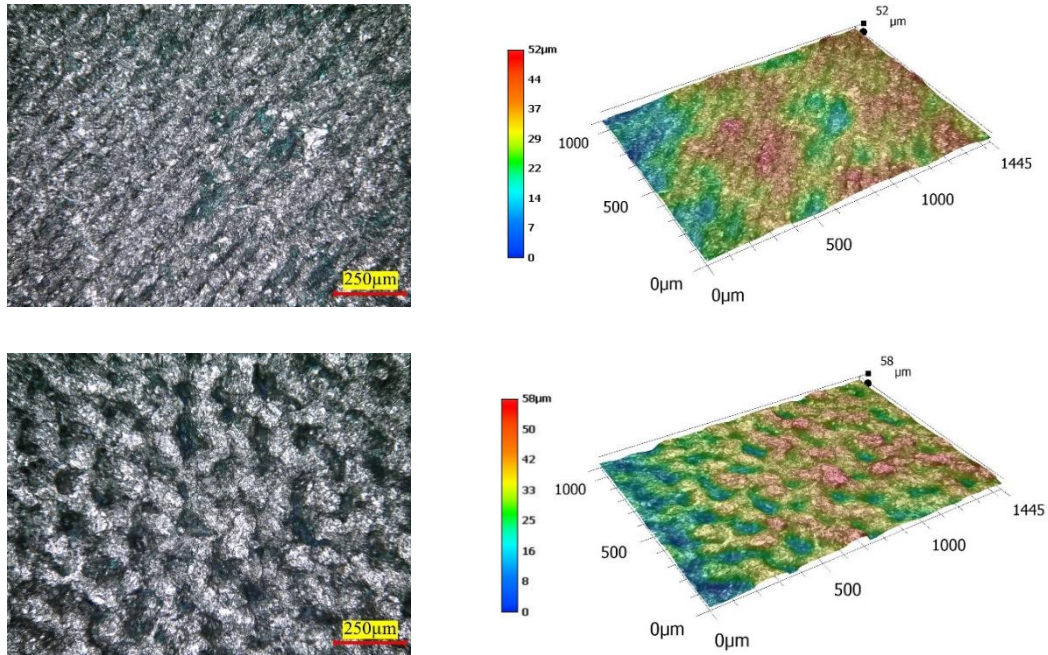


**Figure 2.** Surface topographies in the scanning and building area of the specimens produced by DMLS

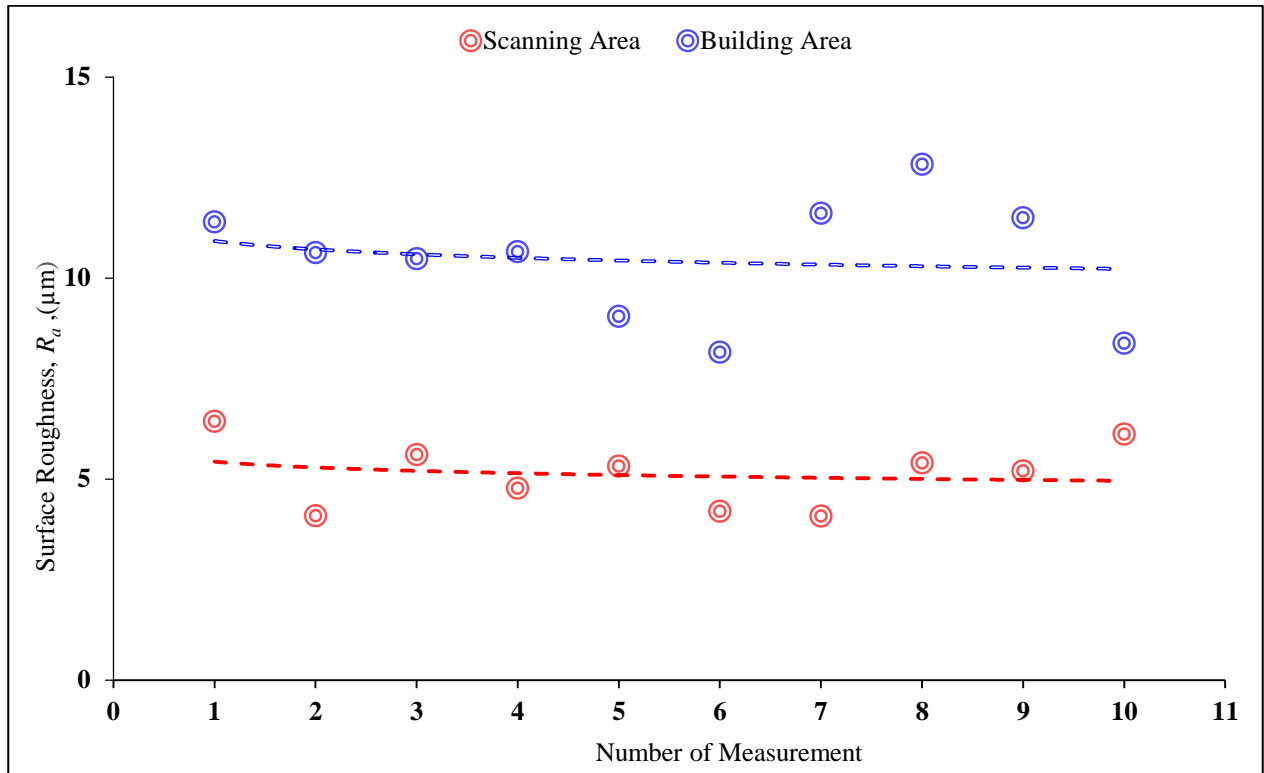


**Figure 3.** Surface roughness values ( $R_a$ ) in the scanning and building area of the specimens produced by DMLS

### 3.2 Microhardness

The hardness values of the specimens were measured on the surface and subsurface. In the literature, the hardness values on the surface are higher than the subsurface, which is explained by the fact that the outer surface is cooled faster than the inner surface [20]. In addition, compared to the production directions (scanning and building area) of the part, the hardness values in the scanning area were found to be higher than the building area due to the anisotropic structure of the part [21-24]. In this current study, the hardness of the wrought maraging steel was measured as 328 ( $\pm 13$ ) HV. Hardness values measured from the scanning and building area of the specimen produced by DMLS were found to be close to each other and mean 570.5 ( $\pm 15$ ) HV. The measured hardness values of the wrought & heat treated maraging steel alloy is 565.8 ( $\pm 9$ ) HV [25]. It is obvious that hardness of specimens fabricated by DMLS is very close to the hardness of wrought that is heat treated. It is possible to say that maraging steel specimens produced by additive manufacturing do not make remarkable difference comparing with conventionally manufactured maraging steels in terms of hardness when it is heat treated. Another important finding is that no obvious hardness difference in between the scanning and building area of specimens produced by DMLS is observed. It indicates that heat treatment helps to homogenize microstructure of specimens fabricated by DMLS and thus the hardness throughout the all directions becomes close to each other. This is indeed desired aspect as considering the usage applications of this material.

### 3.3 Microstructure

The microstructure images of the DMLS specimen were examined in scanning and building area and presented in Figure 4. In the Figure, the scan patterns and melt pools are clearly visible. However, heat treatment has also led to a slight loss of melt pool and scan tracks. In Figure 4(c) and 4(d), microstructure of as-received wrought and heat treated wrought maraging steel specimens are also presented. In this images, it is seen that the material has a martensitic structure [26] and the large initial grains are refined within heat treatment.

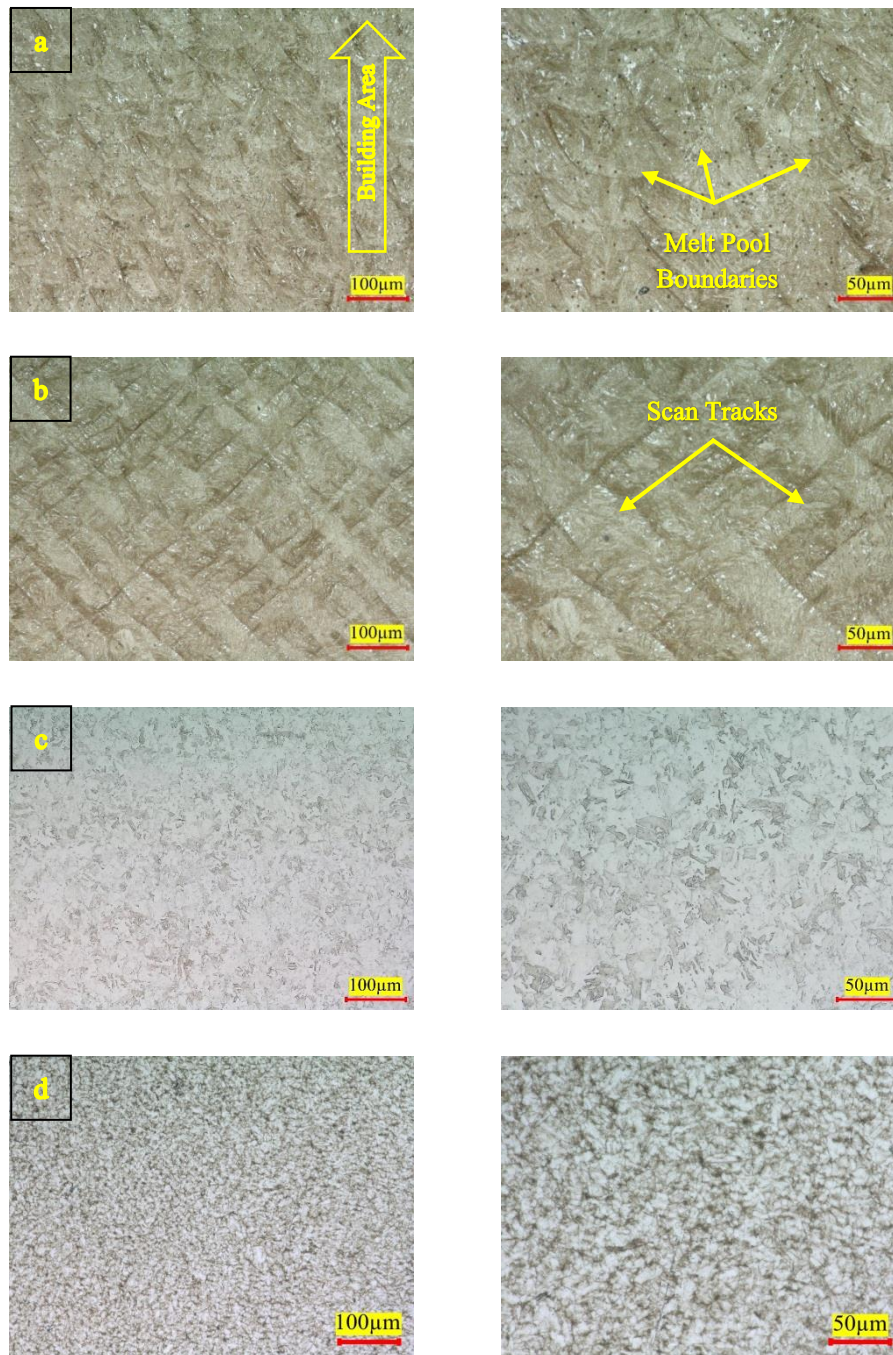


**Figure 4.** Building area of DMLS specimen, (b) Scanning area of DMLS specimen, (c) as-received wrought, (d) heat treated wrought maraging steel

### 3.4 Phase Analysis

Figure 5 shows the XRD patterns of the scanning and building area of the maraging steel. The phase distributions in the Figure consists mainly of martensite phase and partly austenite phases, which is indicate that the microstructures have dual phase in martensite (bcc, body cubic centered) and austenite (fcc, face cubic centered) [26]. In the general distribution, the bcc  $\alpha$ -martensite phase is the dominant phase. Comparing the scanning and building area, it is seen that the peak intensity with ( $\alpha$ -110) is higher in scanning area, however, the peak intensity with ( $\alpha$ -200) texture is higher in the building area. When the as-received wrought and heat treated wrought specimens compared, it can be seen that the grain refinement in the microstructure and increase in the hardness can be explained by increasing the other peak intensity with ( $\alpha$ -110) texture and the other peaks are almost the same. The graph shows that the peak texture intensities in the scanning area could be different due to its crystal

structure and microstructure [27], while in the other specimens at the same peaks. Furthermore, the austenitic phases which is formed beside ( $\alpha$ -110) texture as a result of long-lasting aging heat treatments. This is related the metastable martensite phase with Ni3Ti or Fe2Mo formation transforms into stable austenite phase, which also accelerates austenite transformation [28, 29].

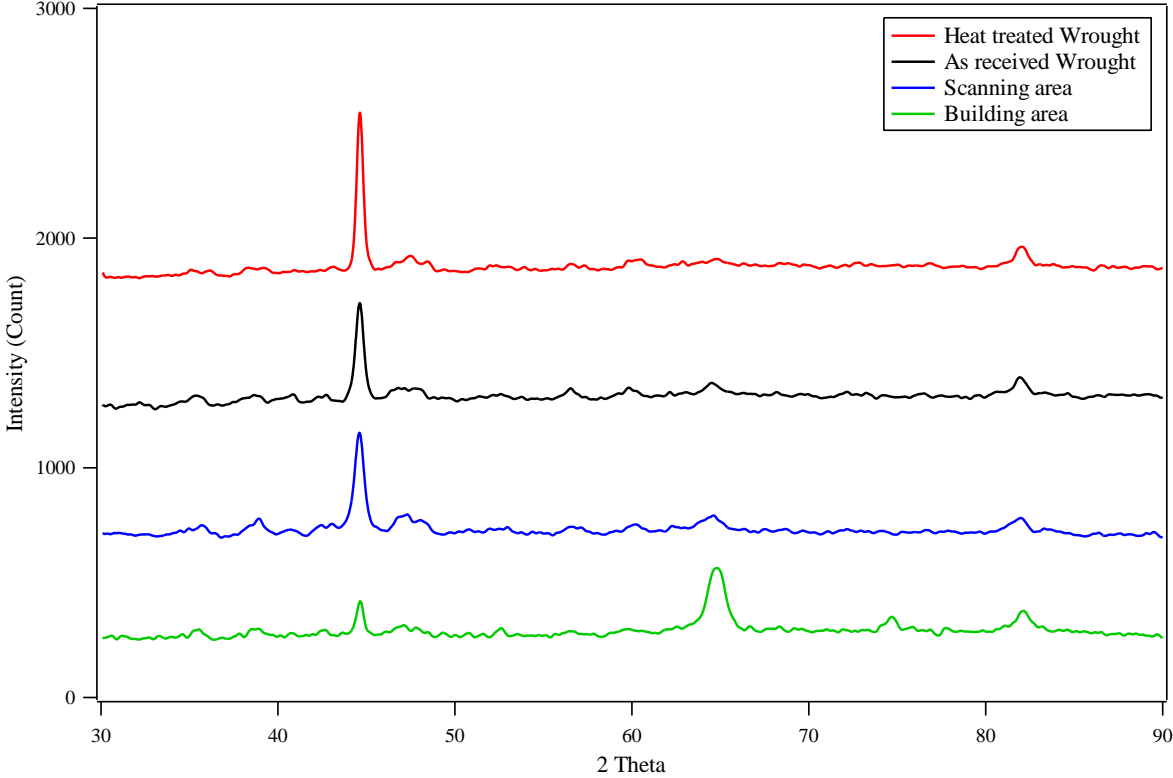


**Figure 5.** XRD peaks of DMLS specimen in the scanning and building area

### 3.5 Wear Resistance

Figure 6 presents the wear response of building and scanning area of specimens produced by DMLS and comparison with the heat treated wrought maraging steel. One of the remarkable contributions of additive manufacturing process seems to be improved wear resistance for this particular material. Indeed, maraging steels have wide range of applications and one of the common applications is die, mold and tooling applications. Thus, wear resistance is a significant indicator to show its performance. Such improvements might be resulting from the residual stress in specimens produced by additive manufacturing [30], which is considered as a factor affecting wear behavior [31, 32]. At the same time, compared to the scanning and building area, the wear depth in the scanning area is slightly higher than the building area.

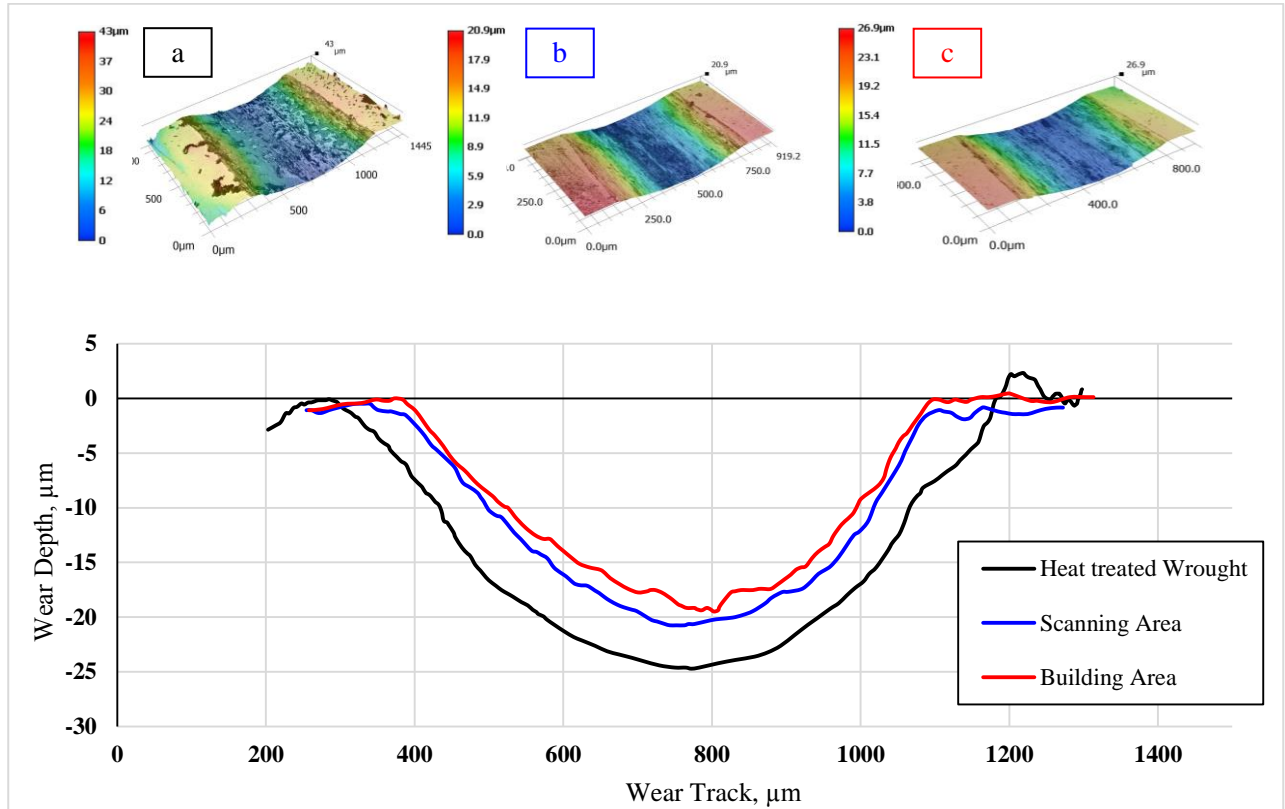


**Figure 6.** 3-D wear topography and corresponding 2-D wear profiles of (a) heat treated wrought, (b) DMLS scanning area, (c) DMLS building area.

The wear rates of the maraging steel specimens produced by the DMLS and the heat treated wrought are illustrated in Figure 7. The wear volume was calculated and analyzed using Equation 1 as shown below [33]:

$$V = L \left[ r^2 \sin^{-1} \left( \frac{w}{2r} \right) - \frac{w}{2} \left( r^2 - \frac{w^2}{4} \right)^{\frac{1}{2}} \right] + \frac{\pi}{3} \left[ 2r^3 - 2r^2 \left( r^2 - \frac{w^2}{4} \right)^{\frac{1}{2}} - \frac{w^2}{4} \left( r^2 - \frac{w^2}{4} \right)^{\frac{1}{2}} \right] \quad (1)$$

where  $V$  equals wear volume in  $\text{mm}^3$ ,  $r$  is the ball radius,  $L$  is the stroke length,  $W$  is the wear-track width and radius of the carbide ball in mm. The wear rate is also as noted below:

$$k = \frac{V}{NxL} \quad (2)$$

where  $k$  is the wear rate in  $\text{mm}^3/\text{Nm}$  and  $N$  is the applied load in Newton.

As shown in Figure 7, the wear rate of the heat treated wrought specimen is much higher than the specimen produced by DMLS process. Scanning area of DMLS specimen has approximately %47 less wear rate than heat treated wrought one, and building area of DMLS specimen has approximately %55 less wear rate than heat treated wrought specimen. These data indicates that parts made of maraging steel produced by laser powder bed fusion process offers much higher wear resistance than the one produced by conventional manufacturing methods.

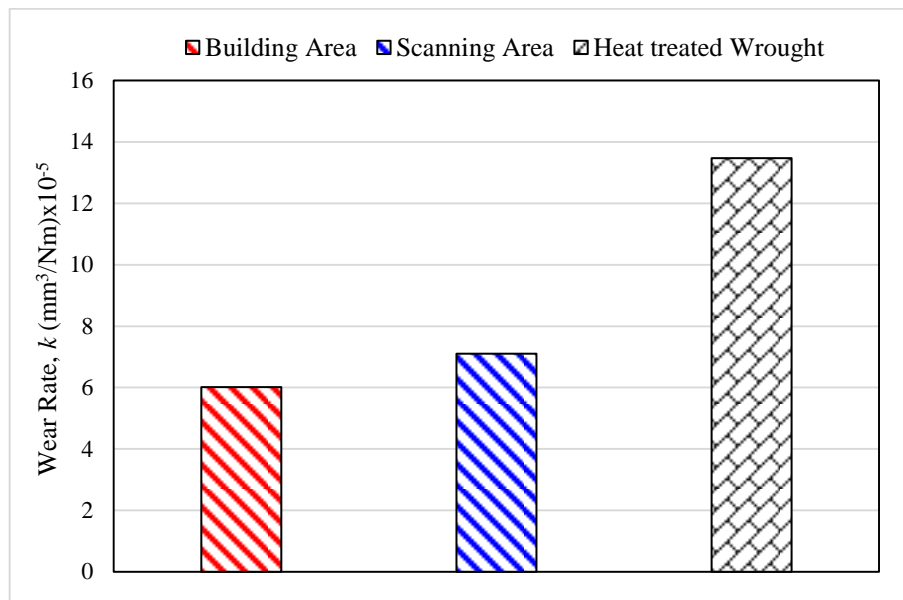


**Figure 7.** Wear rates of DMLS and heat treated wrought specimen.

#### 4. Conclusion

This study focused on the comparison DMLS maraging steel with conventionally manufactured maraging steel in terms of surface integrity aspects and wear resistance. Both specimens namely AM and wrought were heat treated and characterized to compare their performance. This study demonstrates that fabricating maraging steel with DMLS results in improved wear resistance over the conventionally manufactured maraging steels. It is an important advantages considering the various applications of maraging steel. But it should be also noted that there is a negligible difference in between scanning and building area of the specimens in terms of mechanical, surface and wear resistance point of view. Thus, it is possible to reach conclusion that DMLS specimens can be considered as a homogeny throughout the bulk volume after heat treatment process. This is also important point and confirmation considering predictable response of such components under various loading conditions when they are fabricated by DMLS additive manufacturing.

#### Disclaimer

This paper was presented at 18th International Manufacturing Conference in China and pressed in Proceedings of the 18th International Manufacturing Conference in China (IMCC 2019), 09-12 October, 2019, Shenyang, China.

#### References

- [1] DeGarmo, E.P., Black, J.T. & Kohser, R.A. (1997). *Materials and Processes in Manufacturing*. Prentice Hall, 8th Ed., United States of America.
- [2] Jäggle, E. A., Choi, P. P., Van Humbeeck, J. & Raabe, D. (2014). Precipitation and austenite reversion behavior of a maraging steel produced by selective laser melting, *Journal of Materials Research*, 29, 2072-2079.
- [3] Reddy, G.M. & Ramana, P.V. (2012). Role of nickel as an interlayer in dissimilar metal friction welding of maraging steel to low alloy steel, *Journal of Materials Processing Technology*, 212, 66-77.
- [4] Casalino, G., Campanelli, S. L., Contuzzi, N. & Ludovico, A.D. (2015). Experimental investigation and statistical optimisation of the selective laser melting process of a maraging steel, *Optics & Laser Technology*, 65, 151-158.
- [5] Tewari, R., Mazumder, S., Batra, I. S., Dey, G. K. & Banerjee, S. (2000). Precipitation in 18 wt% Ni maraging steel of grade 350, *Acta Materialia*, 48, 1187-1200.
- [6] Thijs, L., Van Humbeeck, J., Kempen, K., Yasa, E., Kruth, J. P. & Rombouts, M. (2011). Investigation on the inclusions in maraging steel produced by Selective Laser Melting. 5th International Conference

- on Advanced Research in Virtual and Rapid Prototyping, 28 September - 1 October 2011, 297-304, Leiria, Portugal.
- [7] Manfredi, D., Ambrosio, E. P., Calignano, F., Krishnan, M., Canali, R., Biamino, S. & Badini, C. (2013). Direct metal laser sintering: an additive manufacturing technology ready to produce lightweight structural parts for robotic applications, *La metallurgia italiana*, 10, 15-24.
- [8] Simchi, A., Petzoldt, F. & Pohl, H. (2003). On the development of direct metal laser sintering for rapid tooling, *Journal of Materials Processing Technology*, 141, 319-328.
- [9] Mumtaz, K. A., Erasenthiran, P. & Hopkinson, N. (2008). High density selective laser melting of Waspaloy®, *Journal of materials processing technology*, 195, 77-87.
- [10] Kaynak, Y. & Kitay, O. (2018). Porosity, surface quality, microhardness and microstructure of selective laser melted 316L stainless steel resulting from finish machining, *Journal of Manufacturing and Materials Processing*, 2, 36.
- [11] Kaynak, Y. & Tascioglu, E. (2018). Finish machining-induced surface roughness, microhardness and XRD analysis of selective laser melted Inconel 718 alloy, *Procedia Cirp*, 71, 500-504.
- [12] Tascioglu, E., Karabulut, Y. & Kaynak, Y. (2020). Influence of heat treatment temperature on the microstructural, mechanical, and wear behavior of 316L stainless steel fabricated by laser powder bed additive manufacturing, *The International Journal of Advanced Manufacturing Technology*, 107, 1947-1956.
- [13] Becker, T. H. & Dimitrov, D. (2016). The achievable mechanical properties of SLM produced Maraging Steel 300 components, *Rapid Prototyping Journal*, 22, 487-494.
- [14] Demir, A. G. & Previtali, B. (2017). Investigation of remelting and preheating in SLM of 18Ni300 maraging steel as corrective and preventive measures for porosity reduction, *The International Journal of Advanced Manufacturing Technology*, 93, 2697-2709.
- [15] 3DSsystems, <https://www.3dsystems.com/3d-printers/prox-dmp-200>. website, 2018: p. 1-1.
- [16] Strano, G., Hao, L., Everson, R. M. & Evans, K.E. (2013). Surface roughness analysis, modelling and prediction in selective laser melting, *Journal of Materials Processing Technology*, 213, 589-597.
- [17] Abstetar, B. (2016) SLM processing-microstructure-mechanical property correlation in an aluminum alloy produced by additive manufacturing, *Graduate Theses & Non-Theses*, 110.
- [18] Li, B. Q., Li, Z., Bai, P., Liu, B. & Kuai, Z. (2018). Research on surface roughness of AlSi10Mg parts fabricated by laser powder bed fusion, *Metals*, 8, 524.
- [19] Jamshidinia, M. & Kovacevic, R. (2015). The influence of heat accumulation on the surface roughness in powder-bed additive manufacturing, *Surface Topography: Metrology and Properties*, 3, 014003.
- [20] Kitay, Ö., Taşcıoğlu, E., Kaş, M., Nesli, Ş., Kaynak, Y. & Yılmaz, O. (2018). Seçici lazerle ergitme yöntemi ile üretilen inconel 625 alaşımlı parçada yüzey bütünlüğünün incelenmesi, 18. Uluslararası Makina Tasarım ve İmalat Kongresi, 3–6 July 2018, Eskişehir, Türkiye.
- [21] Thijs, L., Sistiaga, M. L. M., Wauthle, R., Xie, Q., Kruth, J. P. & Van Humbeeck, J. (2013). Strong morphological and crystallographic texture and resulting yield strength anisotropy in selective laser melted tantalum, *Acta Materialia*, 61, 4657-4668.
- [22] Wu, A. S., Brown, D. W., Kumar, M., Gallegos, G. F. & King, W. E. (2014). An experimental investigation into additive manufacturing-induced residual stresses in 316L stainless steel. *Metallurgical and Materials Transactions A*, 45, 6260-6270.
- [23] Popovich, V. A., Borisov, E. V., Popovich, A. A., Sufiiarov, V. S., Masaylo, D. V. & Alzina, L. (2017). Functionally graded Inconel 718 processed by additive manufacturing: Crystallographic texture, anisotropy of microstructure and mechanical properties, *Materials & Design*, 114, 441-449.
- [24] Yusuf, S. M., Chen, Y., Boardman, R., Yang, S. & Gao, N. (2017). Investigation on porosity and microhardness of 316L stainless steel fabricated by selective laser melting, *Metals*, 7, 64.
- [25] Hokkirigawa, K., Kato, K. & Li, Z.Z. (1988). The effect of hardness on the transition of the abrasive wear mechanism of steels, *Wear*, 123, 241-251.
- [26] Kempen, K., Yasa, E., Thijs, L., Kruth, J. P. & Van Humbeeck, J. (2011). Microstructure and mechanical properties of Selective Laser Melted 18Ni-300 steel, *Physics Procedia*, 12, 255-263.
- [27] Murr, L.E., Martinez, E., Hernandez, J., Collins, S., Amato, K.N., Gaytan, S.M. & Shindo, P.W. (2012). Microstructures and properties of 17-4 PH stainless steel fabricated by selective laser melting, *Journal of Materials Research and Technology*, 1, 167-177.
- [28] Shamantha, C.R., Narayanan, R., Iyer, K.J.L., Radhakrishnan, V.M., Seshadri, S.K., Sundararajan, S. & Sundaresan, S. (2000). Microstructural changes during welding and subsequent heat treatment of 18Ni (250-grade) maraging steel, *Materials Science and Engineering: A*, 287, 43-51.
- [29] Viswanathan, U. K., Dey, G. K. & Asundi, M.K. (1993). Precipitation hardening in 350 grade maraging steel. *Metallurgical Transactions A*, 24, 2429-2442.
- [30] Song, B., Zhao, X., Li, S., Han, C., Wei, Q., Wen, S. & Shi, Y. (2015). Differences in microstructure and properties between selective laser melting and traditional manufacturing for fabrication of metal parts: A review, *Frontiers of Mechanical Engineering*, 10, 111-125.
- [31] Stewart, D.A., Shipway, P.H. & McCartney, D.G. (1998). Influence of heat treatment on the abrasive wear behaviour of HVOF sprayed WC–Co coatings, *Surface and Coatings Technology*, 105, 13-24.

- [32] Mukhopadhyay, A.K. & Yiu-Wing, M. (1993). Grain size effect on abrasive wear mechanisms in alumina ceramics, *Wear*, 162, 258-268.
- [33] Sharma, S.S.K.M.S., Sangal, S. & Mondal, K. (2013). On the optical microscopic method for the determination of ball-on-flat surface linearly reciprocating sliding wear volume, *Wear*, 300, 82-89.